Quantum Mechanical Rate Constants for O + OH ⇌ H + O_2 for Total Angular Momentum $J > 0$

David E. Skinner, Timothy C. Germann, and William H. Miller*

Department of Chemistry, University of California, and Chemical Sciences Division, Lawrence Berkeley National Laboratory, Berkeley, California 94720

Received: January 23, 1998; In Final Form: March 16, 1998

Thermal rate constants have been calculated for the titled reaction for total angular momentum $J > 0$ using the quantum flux correlation function methodology of Thompson and Miller [Thompson, W. H.; Miller, W. H. *J. Chem. Phys.* **1995**, *102*, 7409]. This generalizes earlier work by two of us [Germann,T. C.; Miller, W. H. *J. Phys. Chem. A* **1997**, *101*, 6358] for $J = 0$. A helicity conserving approximation (HCA) is used for the present $J > 0$ calculations, and it and other approximations for treating $J > 0$ are discussed and compared. The results show that for this reaction the much simpler *J*-shifting approximation (JSA) is reasonably accurate (to 10−20% in the rate constants), provided the appropriate choice is made for the reference geometry in this approach.

I. Introduction

In a recent paper,[1] two of us presented the results of rigorous quantum mechanical calculations of the rate constant of the reaction O + OH ⇌ H + O_2 (and also recombination to HO_2 via collisional relaxation by a bath gas). Because of its importance in combustion and atmospheric modeling[2−5] this reaction has been the focus of many studies, *e.g.*, classical trajectory simulations,[6] statistical (RRKM) rate[7] and quantum scattering calculations,[8−11] and also studies of the HO_2 bound[12] and metastable states.[13] Our previous calculations, however, were only carried out explicitly for zero total angular momentum ($J = 0$), the contribution to the rate constant for $J > 0$ being approximated by the "*J*-shifting" approximation (JSA),[14] which assumes that rotational motion is separable from the other degrees of freedom and furthermore that it is that of a rigid rotor (with some assumed geometry). The purpose of the present paper is to report the results of more accurate calculations for $J > 0$, to test the accuracy of the JSA, and see to what extent it is reliable for this reaction. We note that there have been some previous calculations for $J > 0$: those by Wu and Hayes[12] for bound state energy levels of HO_2 for *J* up to 3, and those by Meijer and Goldfield[15] for total reaction probabilities of H + O_2 ($v = 0$, $j = 1$) for $J = 0$, 1, 2, and 5.

How to deal with the $J > 0$ contribution to the thermal rate constants is a nontrivial matter, particularly so for the present reaction which is extremely challenging even for $J = 0$ because of the existence of a long-lived collision complex. At the most rigorous level of theory the quantum mechanical calculation of the rate constant is carried out separately for each value of *J*, and the total rate constant is the sum of those for each *J*,

$$k(T) = \sum_{J=0}^{\infty} (2J+1) k_J(T) \tag{1.1}$$

Typically many values of *J* contribute to this sum, the more so the higher the temperature, and the calculation for each *J* is more difficult than for $J = 0$ because there is an additional coupled degree of freedom. (Matters are not quite so bleak, however, because the *J* dependence of the $k_J(T)$ is usually very simple; one can thus perform the calculation for a few widely spaced values of *J* and then interpolate to evaluate the sum in eq 1.1[16]).

Section II first briefly summarizes the methods used to calculate the rate constant (for each *J*), a fully rigorous quantum mechanical approach based on reactive flux correlation methods.[17,18] Section III then describes the helicity conserving approximation (HCA) used for the present $J > 0$ calculations. A more general HCA is also described in section III, one based on the instantaneous principal axes of the molecular system, and an even wider range of possible approximations for $J > 0$ calculations is also surveyed that may be useful in other applications. The results for the present reaction are presented and discussed in section IV. It is seen that the simplest, JS approximation is not so bad (∼10−20% error) for the present reaction, provided the proper choice is made for the reference geometry.

II. Summary of the Rate Constant Calculation

A. General Theory. Within the HCA (see section III below) the calculation of the rate constant for $J > 0$ is the same as that for $J = 0$ with an effective potential energy surface V_{JK} that depends parametrically on *J* and *K*, the projection of the total angular momentum onto a body-fixed axis. *K* (the helicity) is assumed to be conserved in the HCA, and $k_J(T)$ of eq 1.1 is given by

$$k_J(T) = \sum_{K=-J}^{J} k_{JK}(T) \tag{2.1}$$

where $k_{JK}(T)$ is the result of the rate constant calculation with the effective potential V_{JK}.

The rate constant calculation is carried out as before[1] for each value of *J* and *K*. As discussed there, because the reaction proceeds via a long-lived collision complex, *i.e.*,

$$O + OH \rightleftharpoons HO_2^{\ddagger} \rightarrow H + O_2 \tag{2.2}$$

S1089-5639(98)00872-X CCC: $15.00
Published on Web 05/02/1998

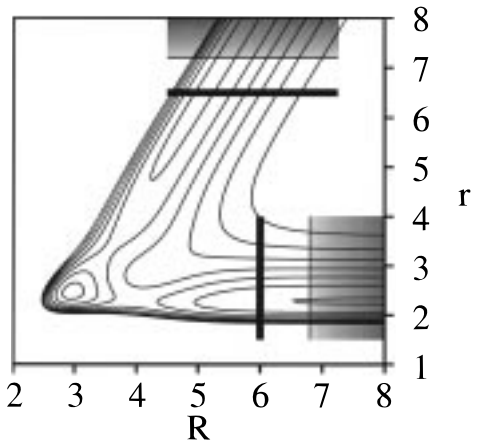

Figure 1. Contour plot of the HO_2 DMBE IV potential energy surface[29] for a colinear ($\gamma = 0$) geometry. The reactant and product dividing surfaces are shown by thick lines. The shaded areas are absorbing potentials $\hat{\epsilon}(R,r)$ which start at the thin lines and increase to the edge of the DVR grid. R and r are shown in atomic units.

it is useful to compute the rate constant as the time integral of a *cross*-correlation function rather than as a flux *auto*correlation function as has been most commonly done in other applications,

$$k(T) = Q_r(T)^{-1}\int_0^\infty dt\, C_{rp}(t) \tag{2.3}$$

where $Q_r(T)$ is the reactant partition function per unit volume and $C_{rp}(t)$ is given by,

$$C_{rp}(t) = tr[e^{-\beta\hat{H}/2}\hat{F}_r e^{-\beta\hat{H}/2} e^{i\hat{H}t/\hbar}\hat{F}_p e^{-i\hat{H}t/\hbar}] \tag{2.4}$$

Here the flux operators, $\hat{F}_r$ and $\hat{F}_p$, are defined with respect to two different dividing surfaces, one on the reactant(O$\cdots$OH) side of the $HO_2^{\ddagger}$ complex region and the other on the product(H + O_2) side, respectively; see Figure 1. (For simplicity of presentation, the Hamiltonian in eq 2.4, and elsewhere in Sections IIa and b, is not labeled by the specific (J, K) value of the calculation.)

The most efficient way we have yet developed for evaluating these flux correlation functions is that described by Thompson and Miller,[19] which has been used before for the O + HCl → OH + Cl[20] and Cl + H_2 → HCl + H[16] reactions, as well as our earlier $J = 0$ calculations for the present reaction.[1] (One should also see the work of Light *et al.*[21] and Matzkies and Manthe[22] which has features similar to our approach.) The first step in this approach is a Lanczos iteration calculation[23] to find the relatively small number of nonzero eigenvalues λ_i and corresponding eigenvectors $|v_i\rangle$ of the Boltzmannized flux operator

$$\hat{F}_r(\beta) = e^{-\beta\hat{H}/2}\hat{F}_r e^{-\beta\hat{H}/2} \tag{2.5a}$$

which can then be represented as

$$\hat{F}_r(\beta) = \sum_i \lambda_i |v_i\rangle\langle v_i| \tag{2.5b}$$

The Lanczos procedure is particularly efficient because $\hat{F}_r(\beta)$ is of low rank, *i.e.*, has a small number of nonzero eigenvalues (approximately twice the number of thermally accessible states on the reactant dividing surface). Figure 2 shows the positive eigenvalues of $\hat{F}_r(\beta)$ for temperatures $T = 600$ and 1000 K, showing how the number increases with T. (The eigenvalues occur in ± pairs, with the eigenvector of the negative eigenvalue being the complex conjugate of that for the positive eigenvalue.)[24,25] The trace in eq 2.4 is then evaluated in the basis of these eigenvectors, giving

$$k(T) = Q_r(T)^{-1}\sum_i \lambda_i \int_0^\infty dt\, \langle v_i(t)|\hat{F}|v_i(t)\rangle \tag{2.6}$$

where $|v_i(t)\rangle$ is the time-evolved vector

$$|v_i(t)\rangle = e^{-i\hat{H}t/\hbar}|v_i\rangle \tag{2.7}$$

We used the split operator algorithm to carry out this time evolution, though other methods for wave packet propagation could also be used.

We note that the general principle in this type of calculation is to choose the dividing surface at the position for which $\hat{F}(\beta)$ will be of the lowest rank possible, so as to minimize the number of vectors which must be time evolved (eq 2.7). This will typically (but may not always) be the dividing surface through the highest energy transition state, *e.g.*, $\hat{F}_r$ in Figure 1. This feature of the procedure is very reminiscent of the variational character of transition state theory,[26] where one chooses the dividing surface to minimize the number of states of the activated complex. In the present (fully dynamical) approach the final result for the rate constant is *formally* independent of where the dividing surface(s) is(are) located but the *efficiency* of the calculation is not.

B. Computational Specifics. A discrete variable representation[27] (DVR) basis was used to represent the wave function at a set of grid points. The underlying finite basis consists of Fourier functions in the r and R coordinates and associated Legendre functions in the γ coordinate. A basis set using 64 × 128 × 32 grid points in the R,r,γ coordinates, respectively, was found to be adequate for the present calculations.

Both the thermal and real time propagation was carried out using the following split-operator[28] factorization of the full quantum propagator,

$$e^{-i(\hat{H}-i\hat{\epsilon})\Delta t} \simeq e^{-i(\hat{V}-i\hat{\epsilon})\Delta t/2}\, e^{-i\hat{T}_\gamma\Delta t/2}\, e^{-i\hat{T}_R\Delta t}\, e^{-i\hat{T}_r\Delta t}\, e^{-i\hat{T}_\gamma\Delta t/2}\, e^{-i(\hat{V}-i\hat{\epsilon})\Delta t/2} \tag{2.8}$$

which expresses (with $\hbar = 1$) the full propagator as a series of one-dimensional kinetic energy operators which can be applied efficiently within the DVR formulation. In order to apply each operator, one transforms to a basis in which the operator is diagonal. For r and R these are Fourier transforms and for γ Legendre transforms. Denoting these transformations as unitary matrices one has

$$\hat{T}_R = \hat{U}_{FFT}^{\dagger}\, \mathrm{diag}\left(\frac{-\hbar^2(j - N_R/2)}{2\mu\Delta R^2}\right)\hat{U}_{FFT} \tag{2.9a}$$

$$\hat{T}_r = \hat{U}_{FFT}^{\dagger}\, \mathrm{diag}\left(\frac{-\hbar^2(j - N_r/2)}{2m\Delta r^2}\right)\hat{U}_{FFT} \tag{2.9b}$$

$$\hat{T}_\gamma = \hat{U}_{Leg}^{\dagger}\, \mathrm{diag}\left(-\hbar^2 J(J+1)\left(\frac{1}{2\mu R^2} + \frac{1}{2mr^2}\right)\right)\hat{U}_{Leg} \tag{2.9c}$$

where diag is a matrix with only diagonal entries (indexed by j), N_R and N_r are 64 and 128 respectively, and $\hat{U}_{Leg}$ is the Legendre transformation which includes the first 32 odd associated Legendre polynomials. (Only odd Legendre polynomials in $cos(\gamma)$ are included because the wave functions must be odd under interchange of the two identical oxygen atoms.[29])

A time step $\Delta t = 10$ au was used for the thermal propagation and 20 au for the real time propagation. For all calculations

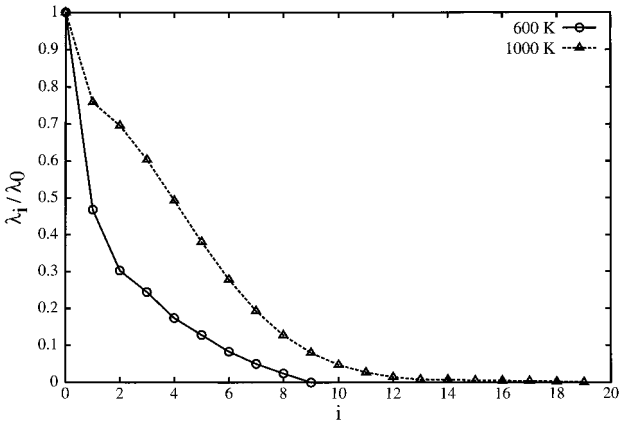

Figure 2. The positive thermal flux eigenvalues at 600 K and 1000 K for $J = 0$ for the dividing surface at the O···OH transition state.

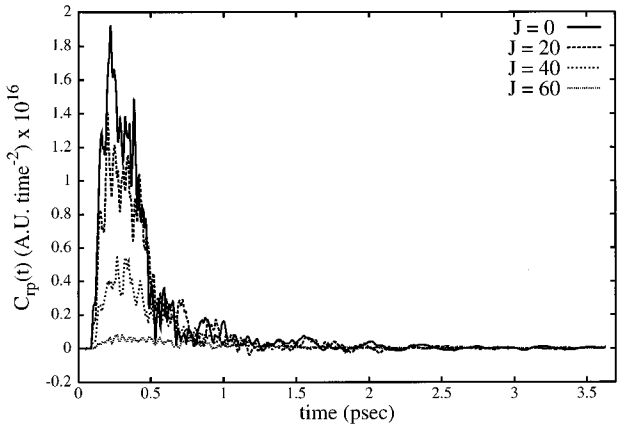

Figure 3. The cross correlation function $C_{fp}(t)$ for several values of J.

the number of thermal flux eigenvectors included is determined by the temperature alone. At $T = 600$ K 20 eigenvectors were propagated and at $T = 1000$ K 40 eigenvectors were propagated. The real-time propagation of the eigenvectors is the most time consuming part of the calculation. These calculations were carried out on a Cray T3D parallel computer and required approximately 1 h/eigenvector in the 64 processor queue.

The dividing surface for reactants (O + OH) is defined by $r = 6.5\ a_0$ and that for products (H + O_2) by $R = 6\ a_0$. The same dividing surfaces were used for all calculations. As in several other studies of HO_2 we use the DMBE IV potential energy surface of Pastrana *et al.*[30] for our calculations.

Absorbing potentials $\hat{\epsilon}(q)$ were placed just beyond each of these dividing surfaces to prevent reflection of reactive flux from the edge of the DVR basis. The reactant and product absorbing potentials start at $r = 7.2\ a_0$ and $R = 6.8\ a_0$, respectively. Both are quartic potentials which rise from zero to a maximum of 0.3 to 0.5 eV. Figure 1 shows a schematic of the dividing surfaces and absorbing potentials.

Figure 3 shows typical results for the flux correlation function, here for $T = 600$ K and for several values of total J. The ~1 ps time scale for the decay of the correlation function, *i.e.*, the lifetime of the collision complex, is seen not to vary much with J.

III. Approximate Treatments for $J > 0$

A. The Helicity Conserving Approximation. Figure 4 shows the Jacobi coordinates that we use—**r** is the O−O coordinate and **R** is that of H and the center of mass of O−O—in terms of which the Hamiltonian has the standard form

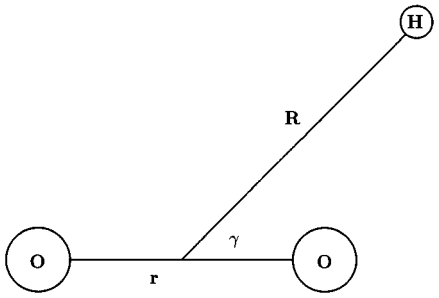

Figure 4. The Jacobi coordinates for the molecular system.

$$\hat{H} = \hat{T}_R + \hat{T}_r + \frac{\hat{l}^2}{2\mu R^2} + \frac{\hat{j}^2}{2mr^2} + V(R,r,\gamma) \qquad (3.1)$$

where

$$\hat{T}_R = -\frac{\hbar^2}{2\mu}\frac{\partial^2}{\partial R^2}, \quad \hat{T}_r = -\frac{\hbar^2}{2m}\frac{\partial^2}{\partial r^2}$$

$\hat{l}$ and $\hat{j}$ are the angular momentum operators for the R and r angular motion, respectively, and V is the potential energy surface. The usual helicity (or j_z) conserving approximation[31] is to choose **R** as the body-fixed quantization axis and to assume that the projection of total angular momentum along it is conserved, *i.e.*, to neglect off-diagonal matrix elements in the quantum number K, the projection quantum number for this body-fixed axis.

This would be a poor choice for the present reaction, however, because the kinematics of the light H atom makes this component of the total angular momentum poorly conserved during the dynamical motion. Choosing the best body-fixed axis for purposes of making a helicity conserving approximation, *i.e.*, neglect of $\Delta K \neq 0$ matrix elements, is the same choice microwave spectroscopists make in deciding on the best "almost symmetric top" axis for molecular rotation;[32] *e.g.*, if the body-fixed axis were indeed a symmetric top axis, then K would be conserved without approximation. From these considerations it is clear that because of the light mass of the H atom a much better, *i.e.*, nearly symmetric top, choice for the body-fixed axis is the O−O axis, *i.e.*, the vector **r**. This idea of using the heavy atom axis in a "heavy + light-heavy" mass combination has often been used in the past,[33] the analogy of the electron in H_2^+ often being invoked. We also note that it was used by Thompson and Miller in their treatment[20] of the O + HCl → OH + Cl reaction.

With **r** thus chosen as the body-fixed axis, one follows Van Vleck's prescription and uses total angular momentum conservation to eliminate the angular momentum for this axis ($\hat{j}$).

$$\hat{j} = \hat{\mathbf{J}} - \hat{l} \qquad (3.2)$$

so that the Hamiltonian becomes

$$\hat{H} = \hat{T}_R + \hat{T}_r + \frac{\hat{l}^2}{2\mu R^2} + \frac{|\hat{\mathbf{J}} - \hat{l}|^2}{2mr^2} + V \qquad (3.3)$$

The HCA is obtained by taking the part of the Hamiltonian diagonal in K, which gives

$$\hat{H}_{JK} = \hat{H}_{J=0} + E_{JK}(R,r,\gamma) \qquad (3.4a)$$

where

$$\hat{H}_{J=0} = \hat{T}_R + \hat{T}_r + \hat{T}_\gamma + V(R,r,\gamma) \qquad (3.4b)$$

with

$$\hat{T}_\gamma = -\hbar^2\left(\frac{\partial^2}{\partial\gamma^2} + \cot\gamma\frac{\partial}{\partial\gamma}\right)\left(\frac{1}{2\mu R^2} + \frac{1}{2mr^2}\right) \quad (3.4c)$$

and

$$E_{JK}(R,r,\gamma) = \frac{J(J+1) - 2K^2}{2mr^2} + \frac{K^2}{\sin^2\gamma}\left(\frac{1}{2\mu R^2} + \frac{1}{2mr^2}\right) \quad (3.4d)$$

The effective potential energy surface for $J > 0$ alluded to in section II is thus

$$V_{JK}(R,r,\gamma) = V(R,r,\gamma) + E_{JK}(R,r,\gamma) \quad (3.5)$$

the actual potential plus a centrifugal potential that is the rotational energy of the molecular complex as a function of the coordinates (R,r,γ) that determine its shape. We note that E_{JK} can also be written in standard symmetric top form,

$$E_{JK}(R,r,\gamma) = B(R,r,\gamma)(J(J+1) - K^2) + C(R,r,\gamma)K^2 \quad (3.6a)$$

where the rotational "constants" are (with $\hbar = 1$)

$$B(R,r,\gamma) = \frac{1}{2mr^2} \quad (3.6b)$$

$$C(R,r,\gamma) = \left(\frac{1}{2\mu R^2} + \frac{\cos^2\gamma}{2mr^2}\right)/\sin^2\gamma \quad (3.6c)$$

B. The *J*-Shifting Approximation. The J-shifting approximation (JSA) results by assuming that the rotational constants in eq 3.6 are truly constants,

$$B(R,r,\gamma) \rightarrow B^\ddagger \equiv B(R^\ddagger,r^\ddagger,\gamma^\ddagger) \quad (3.7a)$$

$$C(R,r,\gamma) \rightarrow C^\ddagger \equiv C(R^\ddagger,r^\ddagger,\gamma^\ddagger) \quad (3.7b)$$

corresponding to some reference geometry $(R^\ddagger,r^\ddagger,\gamma^\ddagger)$. Since the Hamiltonian for $J > 0$ then only differs from that of $J = 0$ by a constant, it is easy to see that the equations in section II lead to

$$k_{JK}(T) = k_{J=0}(T)\mathrm{e}^{-\beta E^\ddagger_{JK}} \quad (3.8a)$$

where

$$E^\ddagger_{JK} = B^\ddagger(J(J+1) - K^2) + C^\ddagger K^2 \quad (3.8b)$$

The sums over J and K in eqs 1.1 and 2.1 then give

$$k(T) = k_{J=0}(T)Q^\ddagger_{\mathrm{rot}} \quad (3.8c)$$

where $Q^\ddagger_{\mathrm{rot}}$ is the rotational partition function,

$$Q^\ddagger_{\mathrm{rot}} = \sum_{J=0}^{\infty}(2J+1)\sum_{K=-J}^{J}\mathrm{e}^{-\beta E^\ddagger_{JK}} \quad (3.8d)$$

which is usually accurately approximated by its classical limit

$$Q^\ddagger_{\mathrm{rot}} = \frac{kT}{B^\ddagger}\sqrt{\frac{\pi kT}{\mathrm{C}^\ddagger}} \quad (3.8e)$$

if $B^\ddagger$ and $\mathrm{C}^\ddagger \leq kT$.

At the level of the JS approximation it is not neccessary to assume that the rigid molecular system has a symmetric top geometry. If it is that of an asymmetric rotor, *i.e.*, all three rotational constants, $A^\ddagger$, $B^\ddagger$, and $C^\ddagger$ are different, then the classical partition function of eq 3.8e becomes

$$Q^\ddagger_{\mathrm{rot}} = \sqrt{\frac{\pi(kT)^3}{A^\ddagger B^\ddagger C^\ddagger}} \quad (3.8f)$$

which can be thought of as the same as the symmetric top expression eq 3.8e with the replacement $B^\ddagger \rightarrow \sqrt{A^\ddagger B^\ddagger}$.

C. Principal Axis Helicty Conserving Approximation. For the present molecular system the O−O axis **r** is a very nearly symmetric top axis because of the lightness of the H atom, but in other cases it may be that neither **R** nor **r** is a good choice. Thus some years ago McCurdy and Miller[34] suggested using one of the instantaneous principal axes of the molecular system as the body-fixed axis for purposes of making a HC approximation. This was motivated by the way microwave spectroscopists[32] make the "best symmetric top" approximation for molecular rotation and also by the desire to have a body-fixed axis that changes continuously from reactants to products during a chemical reaction.

McCurdy and Miller used the classical form of the Hamiltonian, obtained by taking the classical limit of the quantum Hamiltonian operator given by Diehl[35] *et al.*,

$$H(R,p_R,r,p_r,\gamma,p_\gamma,K,q_K) = \frac{1}{2\mu}(p_R - \Delta p_R)^2 + \frac{1}{2m}(p_r - \Delta p_r)^2 + \left(\frac{1}{2\mu R^2} + \frac{1}{2mr^2}\right)(p_\gamma - \Delta p_\gamma)^2 + V(R,r,\gamma) + \frac{J_1^2}{2I_1} + \frac{J_2^2}{2I_2} + \frac{J_3^2}{2I_3} \quad (3.9)$$

where q_K is the angle variable conjugate to the projection "quantum number" (actually action variable) K, and the other coordinates and moments are as before. J_i, $i = 1$, 2, and 3, are the components of the angular momentum along the three instantaneous principal axes, and I_i are the corresponding principal moments of inertia, ordered so that $I_1 < I_2 < I_3 = I_1 + I_2$ (for this planar molecular system); specifically

$$I_2 - I_1 = \sqrt{(\mu R^2)^2 + (mr^2)^2 + 2\mu R^2 mr^2\cos(2\gamma)} \quad (3.10a)$$

$$I_2 + I_1 = \mu R^2 + mr^2 \quad (3.10b)$$

The vibrational angular momentum terms Δp_R, Δp_r, and Δp_γ in eq 3.9 are given by

$$\Delta p_R = -J_3\frac{2I_1I_2}{(I_2 - I_1)^2}\frac{\cos\gamma}{R} \quad (3.11a)$$

$$\Delta p_r = J_3\frac{2I_1I_2}{(I_2 - I_1)^2}\frac{\cos\gamma}{r} \quad (3.11b)$$

$$\Delta p_\gamma = -J_3\frac{2I_1I_2}{(I_2 - I_1)^2}\frac{(\mu R^2 - mr^2)\sin\gamma}{I_1 + I_2} \quad (3.11c)$$

and if principal axis 1 (the one with the smallest moment of inertia) is chosen as the body-fixed quantization axis, then

$$J_1 = K \quad (3.12a)$$

$$J_2 = \sqrt{J^2 - K^2}\cos q_K \tag{3.12b}$$

$$J_3 = \sqrt{J^2 - K^2}\sin q_K \tag{3.12c}$$

The classical version of the HC approximation, which corresponds to the quantum prescription of taking the matrix elements of $\hat{H}$ diagonal in K, is obtained by *averaging* the classical Hamiltonian over the angle variable q_k. In doing this, McCurdy and Miller neglected the contribution from the vibrational angular momentum terms, but it is not necessary to do so. The averaging process is straight forward,

$$\langle\cdots\rangle \equiv \frac{1}{2\pi}\int_0^{2\pi} \mathrm{d}_{q_K}\cdots$$

so that

$$\langle K\rangle = K$$

$$\langle \sin q_K\rangle = \langle \cos q_K\rangle = 0$$

$$\langle \sin^2 q_K\rangle = \langle \cos^2 q_K\rangle = {}^1/_2$$

and it is not hard to carry this out to obtain an HC Hamiltonian of the same form as eq 3.4a,

$$H_{JK}(R,p_R,r,p_r,\gamma,p_\gamma) = H_{J=0} + B(R,r,\gamma)(J^2 - K^2) + C(R,r,\gamma)K^2 \tag{3.13}$$

where $H_{J=0}$ is the same as eq 3.4b and here

$$C(R,r,\gamma) = \frac{1}{2I_1} \tag{3.14a}$$

$$B(R,r,\gamma) = {}^1/_4\left(\frac{1}{I_2} + \frac{I_2 + I_1}{(I_2 - I_1)^2}\right) \tag{3.14b}$$

In the limit $\mu R^2 \ll mr^2$ it is not hard to show that the rotational constants in eq 3.14 revert to those in eq 3.6.

D. Some Further Thoughts on $J > 0$ Approximations. The helicity conserving approximations discussed above try to identify a body-fixed axis which is an almost symmetric top axis for the molecular geometries relevant to the dynamics, so that K (the helicity) is conserved during the dynamics, speaking classically, or a good quantum number, speaking quantum mechanically.

From a very different perspective Bowman[36] has suggested using an *adiabatic rotation* (AR) approximation, which would be justified dynamically if the rotational motion, *i.e.*, q_K, classically, were fast compared to the internal (R,r,γ) motion. In this case one proceeds as in the Born−Oppenheimer approximation, *i.e.*, freezes the (R,r,γ) degrees of freedom and solves for the rotational energy levels of the (in general) asymmetric rotor, $E_{J,\tau}(R,r,\gamma)$, as a function of the internal geometry. The Hamiltonian for the internal motion is then

$$\hat{H}_{J\tau} = \hat{H}_{J=0} + E_{J\tau}(R,r,\gamma) \tag{3.15}$$

i.e., of the same form as that for the HCA, eq 3.4 or eq 3.13. In fact, if the asymmetric rotor energy levels are approximated as an almost symmetric top—which is often a very good approximation—then

$$E_{J\tau}(R,r,\gamma) \rightarrow B(R,r,\gamma)(J(J+1) - K^2) + C(R,r,\gamma)K^2 \tag{3.16}$$

which is then identical to the principal axis HC approximation if the vibrational angular momentum terms are neglected (as McCurdy and Miller originally did).

To complete this discussion the range of possible approximations for $J > 0$ it is useful to consider the opposite limit for the rotational motion, namely that it is much *slower* than the internal (R,r,γ) motion. This is the rotational sudden approximation (SA) which has a long history in molecular collision theory.[37] In the present context this would mean freezing the rotational variables (J,K,q_K) in the Hamiltonian eq 3.9, computing the rate constant as a parametric function of these variables, and then averaging that result over the variables for the rotational degrees of freedom. The net rate constant would thus be given by

$$k(T) = \int_0^\infty \mathrm{d}J\, 2J \int_{-J}^{J} \mathrm{d}K \int_0^{2\pi} \frac{\mathrm{d}q_K}{2\pi}\, k(T; J, K, q_k) \tag{3.17a}$$

where $k(T; J, K, q_k)$ is the rate constant computed from the Hamiltonian that depends parametrically on (J, K, q_K):

$$H(J, K, q_K) = H_{J=0} + \frac{J_1^2}{2I_1} + \frac{J_2^2}{2I_2} + \frac{J_3^2}{2I_3} \tag{3.17b}$$

$$= H_{J=0} + \frac{K^2}{2I_1} + (J^2 - K^2)\left(\frac{\cos^2 q_K}{2I_2} + \frac{\sin^2 q_K}{2I_3}\right) \tag{3.17c}$$

where we have for simplicity dropped the vibrational angular momentum terms (they could be retained if desired). This approximation is somewhat more costly to implement than the PA/HCA because the result of the calculation now depends on the three parameters (J, K, q_K) rather than just two, (J, K). In the symmetric top limit, $I_2 \simeq I_3$, however, one sees that the q_K dependence in eq 3.17c disappears and one is again back to the same expression as the PA/HCA. Thus if the internal dynamics is confined to molecular geometries that are well approximated as a symmetric top, one obtains the same effective Hamiltonian whether rotation is treated as fast or slow. Finally, it is easy to show that eq 3.17a for the sudden approximation can be written as

$$k(T) = \frac{1}{2\pi}\int d_3\mathbf{J}\; k(T; \mathbf{J}) \tag{3.18a}$$

with

$$H_{\mathbf{J}} = H_{J=0} + \frac{1}{2}\mathbf{J}\cdot\mathbf{I}(R,r,\gamma)^{-1}\cdot\mathbf{J} \tag{3.18b}$$

which makes it clear that this approximation is completely independent of how the body-fixed axis is chosen; *e.g.*, it is not even necessary in eq 3.18b that the inertia tensor be diagonal. By evaluating the integral over $\mathbf{J}$ in spherical coordinates (J, θ, ϕ),

$$\int \mathrm{d}_3\,\mathbf{J} = \int_0^\infty \mathrm{d}J\, J^2 \int_0^\pi \mathrm{d}\theta\, \sin\theta \int_0^{2\pi} \mathrm{d}\phi \tag{3.19}$$

one can show that eq 3.18a is equivalent to eq 3.17a.

IV. Results and Discussion

The HCA described in section IIIa was used for the $J > 0$ calculations reported here. This should be an excellent approximation for this reaction because the O−O axis is such a good "almost symmetric top" axis; *e.g.*, in Table 1 one sees how close are the two smallest rotational constants $A^\ddagger$ and $B^\ddagger$

TABLE 1: Rotational Constants and Partition Functions at Fixed Geometries

geometry	$A^{\ddagger}/cm^{-1}$	$B^{\ddagger}/cm^{-1}$	$C^{\ddagger}/cm^{-1}$	$Q^{\ddagger}_{rot}$ (600 K)	$Q^{\ddagger}_{rot}$ (1000 K)
HO_2 minimum[a]	1.051	1.115	20.51	3069	6603
O···OH TS[a]	0.286	0.287	44.52	7897	16971
HCA TS[b]	0.290	0.290	45.00	9647	19350

[a] Exact rotational constants of the three atom system at the indicated geometry. [b] Rotational constants of the O···OH geometry implied by the HCA eq 3.6.

TABLE 2: Parameters Describing the Dependence of $k_{JK}(T)$ on J and K in Equation 4.1

temperature/K	a/cm^{-1}	b/cm^{-1}	B/cm^{-1}	C/cm^{-1}
600	−3.14	77.7	0.318	1.65
1000	−2.37	62.7	0.336	18.3

at both the geometry of the HO_2 minimum and the O···OH transition state. One also sees how close are the exact rotational constants of the O···OH transition state and those implied by the HCA (eq 3.6) at this geometry.

Within the HCA, however, the calculation of $k_{JK}(T)$ for each (J, K) is equivalent in effort to the $k_{J=0}(T)$ calculation, which is itself already a very expensive calculation due to the the small grid spacing that is necessary because of the deep potential well and also the long propagation times resulting from the long-lived complex. It is therefore very important to minimize the number of (J, K) values for which calculations are actually performed. To this end the (J, K) dependence of $k_{JK}(T)$ was fit to the following functional form

$$\ln[k_{JK}(T)/k_{00}(T)] = -\beta\{aJ + b|K| + B[J(J+1) - K^2] + CK^2\} \quad (4.1)$$

which is sufficiently accurate for the range of J and K values that contribute. Adding terms of higher order in J and K did not affect to result for the total rate constant. Between 15 and 19 $k_{JK}(T)$ were calculated to perform this fit at each temperature. The values of a, b, B, and C determined from the fit and used for the interpolation are given in Table 2. The sum over J and K to obtain the total rate thus gives the same form as the JSA:

$$k(T) = k_{J=0}(T)Q_{rot}(T) \quad (4.2a)$$

where here

$$Q_{rot}(T) = \sum_{J=0}^{\infty}\sum_{K=-J}^{J} e^{-\beta\{aJ+b|K|+B[J(J+1)-K^2]+CK^2\}} \quad (4.2b)$$

Table 3 lists the rate constants given by the HCA at $T = 600$ and 1000 K, and also those given by the JSA with two possible choices of the reference geometry, that of the HO_2 minimum and that of the O···OH transition state. (Here we note an error in the use of the JSA in our previous paper;[1] the rotational constants used there for the HO_2 minimum—$A^{\ddagger} = 0.572$ cm^{-1}, $B^{\ddagger} = 0.589$ cm^{-1}, $C^{\ddagger} = 18.94$ cm^{-1}—are in error; the correct values are those in Table 1.)

Comparing the (presumably) accurate HCA results with those of the JSA in Table 3, one sees that the JSA is not bad—the rate constant agrees with that of the HCA to 10−20% for this temperature range—*provided* one uses the O···OH transition state as the reference geometry for the rotational motion. For a "direct" reaction it is commonly believed—with some examples to support it[16,38]—that the transition state geometry is the best reference geometry for the JSA, but since the collision complex ($HO_2^{\ddagger}$) spends most of its time in the region about the HO_2 minimum, it was not obvious that this latter geometry might not be a better choice in this case. The minimum *does* seem to be the best choice for the JSA in describing resonance energies[39] of the HCO complex, a very similar system. For the rate constant, however, we see that in this case, too, the transition state geometry is the best choice for the JSA.

TABLE 3: Rate Constants in cm^3 molecule^{-1} s^{-1} for H + O_2 → O + OH

method	$k(600\ K) \times 10^{16}$	$k(1000\ K) \times 10^{14}$
JSA (HO_2 minimum)	1.32	3.52
JSA (O···OH TS)	3.39	9.03
HCA	4.12	10.3
experiment[a]	3.72	9.1

[a] The rate constant at 600 K was extrapolated from a measurement of k^{-1}(520 K) by Howard and Smith[41] using the experimentally determined equilibrium constant.[42] The rate constant at 1000 K was measured by Eberius *et al.*[43]

This latter observation, *i.e.*, that the transition state geometry provides the best choice of reference geometry for the JSA in both "complex-forming" as well as "direct" reactions, is thus an encouraging one, for the JSA is by far the simplest way of dealing with $J > 0$ if the choice of reference geometry is unambiguous. The full dynamical calculation is then required only for $J = 0$, an enormous simplification. It is important, however, to have the possibility of carrying out more accurate treatments of $J > 0$, as discussed in section III, to calibrate its reliability, as in the present application.

Finally, we note from Table 3 that the rate constants given by the HCA (and the JSA with the O···OH reference geometry) with this potential surface are in quite good agreement with the experimental values. To pursue matters further, it would be useful to utilize the more recent and presumably more accurate potential energy surface developed by Kendrick and Pack[40] and also to deal explicitly with the electronically non-adiabatic dynamics arising from the spin−orbit coupling in this system.

Acknowledgment. We thank Claude Leforestier for providing the DMBE IV potential subroutine. This work has been supported by the Director, Office of Energy Research, office of Basic Energy Science, Chemical Sciences Division, of the U.S. Department of Energy under Contract DE-AC03-76SF00098, by the Laboratory Directed Research and Development (LDRD) project from National Energy Research Scientific Computing (NERSC) Center, Lawrence Berkeley Laboratory, and also in part by National Science Foundation Grant CHE-9732758. We acknowledge a grant of Cray T3D computer time from the Advanced Computing Initiative in Science and Engineering (ACISE) at Lawrence Livermore National Laboratory. D. E. Skinner gratefully acknowledges a research fellowship from the Fannie and John Hertz Foundation. T. C. Germann gratefully acknowledges a research fellowship from the Miller Institute.

References and Notes

(1) Germann, T. C.; Miller, W. H. *J. Phys. Chem. A* **1997**, *101*, 6358.

(2) Pilling, M. J.; Seakins, P. W. *Reaction Kinetics*; Oxford University Press: Oxford, 1995; Chapter 10.

(3) Wennberg, P. O.; Cohen, R. C.; Stimpfle, R. M.; Koplow, J. P.; Anderson, J. G.; Salawitch, R. J.; Fahey, D. W.; Woodbridge, E. L.; Keim, E. R.; Gao, R. S.; Webster, C. R.; May, R. D.; Toohey, D. W.; Avallone, L. M.; Proffitt, M. H.; Lowenstein, M.; Podolske, J. R.; Chan, K. R.; Wofsy, S. C. *Science* **1994**, *266*, 398.

(4) Gardiner, W. C. *Combustion Chemistry*; Springer: Berlin, FRG, 1984.

(5) Miller, J. A.; Kee, R. J.; Westbrook, C. K. *Annu. Rev. Phys. Chem.* **1990**, *41*, 345.
(6) Miller, J. A. *J. Chem. Phys.* **1986**, *84*, 6170.
(7) Duchovic, R. J.; Pettigrew, J. D.; Welling, B.; Shipchandler, T. *J. Chem. Phys.* **1996**, *105*, 10367.
(8) (a) Pack, R. T.; Butcher, E. A.; Parker, G. A. *J. Chem. Phys.* **1993**, *99*, 9310. (b) Pack, R. T.; Butcher, E. A.; Parker, G. A. *J. Chem. Phys.* **1995**, *102*, 5998.
(9) (a) Zhang, D. H.; Zhang, J. Z. H. *J. Chem. Phys.* **1994**, *101*, 3671. (b) Dai, J.; Zhang, J. Z. H. *J. Chem. Phys.* **1996**, *104*, 3664. (c) Dai, J.; Zhang, J. Z. H. *J. Phys. Chem.* **1996**, *100*, 6898.
(10) Leforestier, C.; Miller, W. H. *J. Chem. Phys.* **1994**, *100*, 733.
(11) (a) Dobbyn, A. J.; Stumpf, M.; Keller, H.-M.; Hase, W. L.; Schinke, R. *J. Chem. Phys.* **1995**, *102*, 5867. (b) Song, K.; Peslherbe, G. H.; Hase, W. L.; Dobbyn, A. J.; Stumpf, M.; Schinke, R. *J. Chem. Phys.* **1995**, *103*, 8891. (c) Dobbyn, A. J.; Stumpf, M.; Keller, H.-M.; Schinke, R. *J. Chem. Phys.* **1995**, *103*, 9947. (d) Dobbyn, A. J.; Stumpf, M.; Keller, H.-M.; Schinke, R. *J. Chem. Phys.* **1996**, *104*, 8357.
(12) Wu, X. T.; Hayes, E. F. *J. Chem. Phys.* **1997**, *107*, 2705.
(13) Mandelshtam, V. A.; Grozdanov, T. P.; Taylor, H. S. *J. Chem. Phys.* **1995**, *103*, 10074.
(14) Bowman, J. M. *J. Phys. Chem.* **1991**, *95*, 4960.
(15) Meijer, A.; Goldfield, E. Preprint.
(16) Wang, H.; Thompson, W. H.; Miller, W. H. *J. Chem. Phys.* **1997**, *107*, 7194.
(17) Miller, W. H.; Schwartz, S. D.; Tromp, J. W. *J. Chem. Phys.* **1983**, *79*, 4889.
(18) Yamamoto, T. *J. Chem. Phys.* **1960**, *33*, 281.
(19) Thompson, W. H.; Miller, W. H. *J. Chem. Phys.* **1995**, *102*, 9205.
(20) Thompson, W. H.; Miller, W. H. *J. Chem. Phys.* **1997**, *106*, 142.
(21) Park, T. J.; Light, J. C. *J. Chem. Phys.* **1988**, *88*, 4897.
(22) Matzkies, F.; Manthe, U. *J. Chem. Phys.* **1998**, *108*, 4828.
(23) Lanczos, C. *J. Res. Nat. Bur. Stand.* **1950**, *45*, 255.
(24) Park, T. J.; Light, J. C. *J. Chem. Phys.* **1988**, *88*, 4897.
(25) Seideman, T.; Miller, W. H. *J. Chem. Phys.* **1991**, *95*, 1768.
(26) Truhlar, D. G.; Garrett, B. C. *Annu. Rev. Phys. Chem.* **1984**, *35*, 159.
(27) (a) Lill, J. V.; Parker, G. A.; Light, J. C. *Chem. Phys. Lett.* **1982**, *89*, 483. (b) Light, J. C.; Hamilton, I. P.; Lill, J. V. *J. Chem. Phys.* **1985**, *82*, 1400. (c) Lill, J. V.; Parker, G. A.; Light, J. C. *J. Chem. Phys.* **1986**, *85*, 900. (d) Bačić, Z.; Light, J. C. *J. Chem. Phys.* **1986**, *85*, 4594. (e) Whitnell, R. M.; Light, J. C. *J. Chem. Phys.* **1988**, *89*, 3674. (f) Choi, S. E.; Light, J. C. *J. Chem. Phys.* **1990**, *92*, 2129.
(28) (a) Fleck, J. A., Jr.; Morris, J. R.; Feit, M. D. *Appl. Phys.* **1976**, *10*, 129. (b) Feit, M. D.; Fleck, J. A., Jr.; Steiger, A. *J. Comput. Phys.* **1982**, *47*, 412.
(29) The symmetry requirements of the HO_2 wave function are discussed more fully in Barclay, V. J.; Dateo, C. E.; Hamilton, I. P.; Kendrick, B.; Pack, R. T.; Schwenke, D. W. *J. Chem. Phys.* **1995**, *103*, 3864.
(30) Pastrana, M. R.; Quintales, L. A. M.; Brandão, J.; Varandas, A. J. C. *J. Phys. Chem.* **1990**, *94*, 8073.
(31) (a) Pack, R. T. *J. Chem. Phys.* **1974**, *60*, 633. (b) McGuire, P.; Kouri, D. J. *J. Chem. Phys.* **1974**, *60*, 2488.
(32) Townes, C. H.; Schawlow, A. L. *Microwave Spectroscopy*; McGraw-Hill: New York, 1955.
(33) Herschbach, D. *Adv. Chem. Phys.* **1966**, *10*, 319.
(34) McCurdy, C. W.; Miller, W. H. *ACS Symposium Series 56*; Brooks, P. R., Hayes, E. F., Eds.; American Chemical Society: Washington, DC, 1977; pp 239−242.
(35) Diehl, H.; Flügge, S.; Schröder, U.; Völkel, A.; Weiguny, A. *Z. Phys.* **1961**, *162*, 1.
(36) (a) Bowman, J. M. *Chem. Phys. Lett.* **1994**, *217*, 36. (b) Qi, J.; Bowman, J. M. *J. Phys. Chem.* **1996**, *100*, 15165. (c) Qi, J.; Bowman, J. M. *J. Chem. Phys.* **1997**, *107*, 9960.
(37) (a) Kramer, K. H.; Bernstein, R. B. *J. Chem. Phys.* **1964**, *40*, 200. (b) Kramer, K. H.; Bernstein, R. B. *J. Chem. Phys.* **1966**, *44*, 4473.
(38) Wang, D.; Bowman, J. M. *J. Phys. Chem.* **1994**, *98*, 7994.
(39) (a) Qi, J.; Bowman, J. M. *J. Chem. Phys.* **1996**, *105*, 9884. (b) Qi, J.; Bowman, J. M. *Chem. Phys. Lett.* **1997**, *276*, 371.
(40) Kendrick, B.; Pack, R. T. *J. Chem. Phys.* **1995**, *102*, 1994.
(41) Howard, M. J.; Smith, I. W. M. *J. Chem. Soc., Faraday Trans. 2* **1981**, *77*, 997.
(42) Cohen, N.; Westberg, K. R. *J. Phys. Chem. Ref. Data* **1983**, *12*, 531.
(43) Eberius, K. H.; Hoyermann, K.; Wagner, H. G. *Proceedings of the International Thirteenth Symposium International on Combustion*; The Combustion Institute: Pittsburgh, 1971.